

NASA TM-77981

NASA-TM-77981 19860012321

A Reproduced Copy
OF

NASA TM- 77981

Reproduced for NASA
by the
NASA Scientific and Technical Information Facility

LIBRARY COPY

OCT 7 1986

LANGLEY RESEARCH CENTER
LIBRARY, NASA
HAMPTON, VIRGINIA

FFNo 672 Aug 65

NASA TECHNICAL MEMORANDUM

NASA TM-77981

STUDIES OF ACOUSTIC EFFECTS ON A FLOW
BOUNDARY LAYER IN AIR

F. Mechel and W. Schilz

(NASA-TM-77981) STUDIES OF ACCUSTIC EFFECTS
ON A FLOW BOUNDARY LAYER IN AIR [National
Aeronautics and Space Administration] 17 p
HC 102/MF ADI

CSCL 20D

N86-21792

Unclass

G3/34 05726

Translation of "Untersuchungen zur akustischen
Beeinflussung der Strömungsgrenzschicht in Luft," Acustica,
Vol. 14, 1964, pp. 325-331



NATIONAL AERONAUTICS AND SPACE ADMINISTRATION
WASHINGTON, D.C. 20546 FEBRUARY 1986

N86-21792 #5

ORIGINAL PAGE IS
OF POOR QUALITY

STANDARD TITLE PAGE

1. Report No. NASA TM-77981	2. Government Accession No.	3. Recipient's Catalog No.	
4. Title and Subtitle STUDIES OF ACOUSTIC EFFECTS ON A FLOW BOUNDARY LAYER IN AIR		5. Report Date February 1986	
6. Author(s) F. Mechel and W. Schilz, 3rd Physical Institute, University of Göttingen		7. Performing Organization Code	
8. Performing Organization Name and Address Leo Kanner Associates, Redwood City, CA 94063		9. Performing Organization Report No.	
10. Work Unit No.		11. Contract or Grant No. NASW-4005	
12. Sponsoring Agency Name and Address National Aeronautics and Space Administration, Washington, D.C. 20546		13. Type of Report and Period Covered Translation	
14. Sponsoring Agency Code			
15. Supplementary Notes <p>Translation of "Untersuchungen zur akustischen Beeinflussung der Strömungsgrenzschicht in Luft," Acustica, Vol. 14, 1964, pp. 325-331.</p>			
16. Abstract <p>Effects of sound fields on the flow boundary layer on a flat plate subjected to a parallel flow are studied. The boundary layer is influenced by controlling the stagnation point flow at the front edge of the plate. Depending on the Reynolds number and sound frequency, excitation or suppression of turbulence is observed. Measurements were taken at wind velocities between 10 and 30 m/sec and sound frequencies between 0.2 and 3.0 kHz.</p>			
17. Key Words (Selected by Author(s))	18. Distribution Statement Unclassified--Unlimited		
19. Security Classif. (of this report) Unclassified	20. Security Classif. (of this page) Unclassified	21. No. of Pages 17	22.

STUDIES OF ACOUSTIC INFLUENCE ON A FLOW
BOUNDARY LAYER IN AIR

F. Mechel and W. Schilz
Third Physical Institute of the University of Göttingen

Summary

1325*

The effects of sound fields on the flow boundary layer on a flat plate subjected to a parallel flow are studied. The boundary layer is influenced by controlling the stagnation point flow at the front edge of the plate.

Depending on the Reynolds number (wind velocity) and the sound frequency, an excitation or suppression of boundary-layer turbulence is observed.

The measurements were taken at wind velocities of 10 to 30 m/s and sound frequencies between 0.2 and 3.0 kHz.

1. Introduction

The possibility of acoustically influencing flows has been known since the experiments on sound-sensitive flames first conducted by LeConte [1] in 1858. Those and subsequent studies on this problem involved the effects of sound fields on the development of turbulence in a free jet. (A list including the most important literature appears in a publication of Chanaud and Powell [2].)

The present paper provides some investigations of acoustic influences on the plate boundary layer, with the interaction

*Numbers in the margin indicate pagination in the foreign text.

between sound field and flow occurring in the stagnation point at the front edge of the plate. At various sound frequencies, both an excitation and a suppression of turbulence are observed.

Symbols

V	Flow rate
V_∞	Flow rate in outer flow
V_0	Flow rate before stagnation point
v	Alternation velocity
x	Position coordinate in direction of flow <u>326</u>
y	Position coordinate perpendicular to direction of flow, $x = y = 0$: stagnation point
A	Sound alternation amplitude at stagnation point
$\omega = 2\pi f$	Angular frequency
t	Time
$k = (\beta + j\alpha)$	Complex wave number
δ	Boundary layer thickness
δ^*	Displacement thickness
ν	Kinematical viscosity
b	Parameter of stagnation point profile

2. Measurement Setup

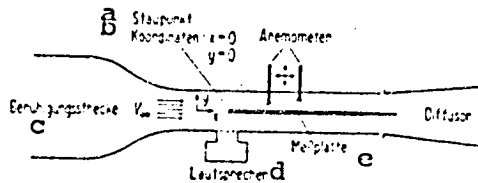
Acoustic influence on boundary layers was studied in a wind tunnel with a free cross section of 10 cm x 10 cm. To obtain an untrammelled flow in the test section, the air flow, supplied by a radial blower, was first cleared of interfering noise in a noise damper, and then passed through a turbulence smoothing section and a contraction horn (ratio 25:1) to the test section. The degree of turbulence of the free flow in the test section is less than 5×10^{-4} in the velocity range between 5 and 30 m/s. The test section concludes with an 8° diffusor.

The structure of the test section is diagrammed in Fig. 1. The channel is divided into two equal halves by a horizontal plate 3 mm thick. The front edge of the plate is rounded with a radius of curvature of 1.5 mm. Under the front edge is the gauze-covered inlet for the sound signal, generated by a 12 W pressure chamber system.

Fig. 1. Diagram of measurement setup.

Key:

- a. stagnation point
- b. coordinates
- c. smoothing section
- d. loudspeaker
- e. measurement plate



Two hot-wire anemometers (DISA constant temperature anemometers), which can move vertically and horizontally, serve to measure the flow and the boundary layer perturbations.

3. Approximations for Profile Control

A sound signal superposed on the flow influences the development of the flow boundary layer along the plate, by controlling the stagnation point profile at the front edge of the plate. Since the arrangement in the vicinity of the stagnation point selected here primarily produces a vertical particle velocity, sound and flow can easily be superposed. The distribution of velocities with a fixed x coordinate ahead of the stagnation point is approximated by the following equation:

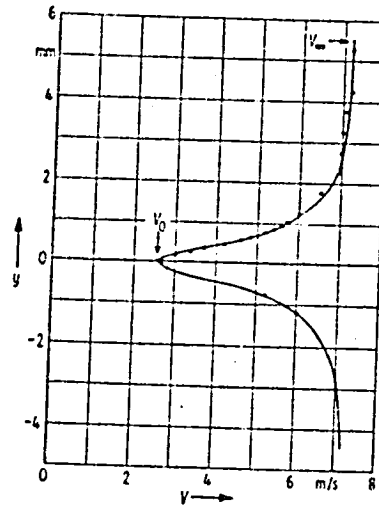
$$U = U_\infty - \frac{U_\infty - U_0}{1 + b y^2}. \quad (1)$$

Figure 2 shows good agreement between the measurement points and the velocity profile thus calculated.

The linear superposition of a particle velocity in the y direction is introduced in Eq. 1 by replacing y with $(y +$

Fig. 2. Measured velocity distribution 1 mm ahead of stagnation point, compared to calculated approximation.

○○○ measurement points
— curve calculated with Eq. (1).



$A \sin \omega t$), where A is the sound alternation amplitude. With this we get:

$$V = V_\infty - \frac{V_\infty - V_0}{1 + b(y + A \sin \omega t)^2}. \quad (2)$$

Assuming that $b A \frac{A + 2y}{1 + by^2} \ll 1$, and neglecting the terms of greater than second order, for the x component of the resulting flow one gets:

$$V = V_\infty \left[1 - \frac{1 - V_0/V_\infty}{1 + b y^2} \left(1 - \frac{b A^2}{2(1 + b y^2)} - b \frac{4y A \sin \omega t - A^2 \cos 2\omega t}{2(1 + b y^2)} \right) \right]. \quad (3)$$

Here the alternating velocity induced by sound control is /327

$$v = \frac{(V_\infty - V_0) b}{2(1 + b y^2)^2} A (4y \sin \omega t - A \cos 2\omega t). \quad (4)$$

This alternating velocity contains both the frequency ω and the first harmonic 2ω . Both components decrease rapidly as y increases. They are limited to the immediate vicinity of the stagnation point. In the transition from positive to negative y

values, the phase of the fundamental jumps 180° while that of the harmonic remains constant.

The superposition of these two components generates periodically occurring rotational fields at the stagnation point, whose points of rotation are not in the plane $y = 0$. Figure 3 shows a section of the profile of the alternating velocity under Eq. (4) for the two phases $\omega t = \pi/2$ and $3\pi/2$. In each period a laevo-rotational field is generated above and a dextrorotational field is generated below the line $y = 0$. These rotational fields can now excite vortices which then, depending on the position of the centers, are guided along the top or bottom of the plate and help form boundary layer waves.

Fig. 3. Development of rotational fields in the stagnation point by acoustic superposition.

Key:
 a. alternating velocity
 b. wavelength of perturbation

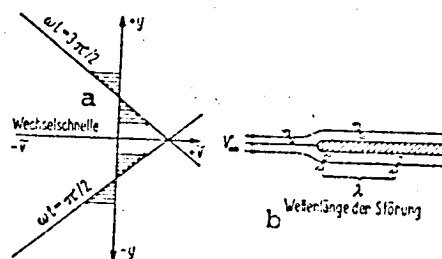


Figure 4 shows a comparison of the alternating velocity calculated by Eq. (4) with the measured velocity distribution ahead of the stagnation point. The calculation is based on the experimentally determined stagnation point profile (Fig. 2). The solid line is calculated; the points are measured values. The values were derived from the total alternating velocity by subtracting the particle velocity (the amplitude and direction distribution of the particle velocity was measured in still air). The amplitude factor A appearing in Eq. (4) was determined by measurement. The approximation condition is satisfied by:

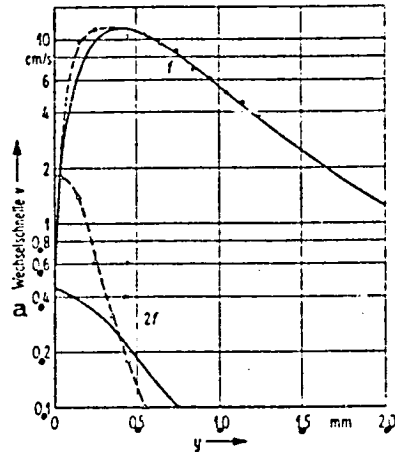
$$b \cdot A \frac{A + 2y}{1 + b y^2} \leq 3.5 \times 10^{-2}$$

ORIGINAL PAGE IS
OF POOR QUALITY.

Fig. 4. Measured and calculated amplitude of alternating velocity 1 mm ahead of the stagnation point.

$\circ \text{---} \circ$ } measured
 $\Delta \text{---} \Delta$ } calculated

Key: a. alternating velocity



The relatively poor agreement between the absolute values for $2f$ and the measurements may be due to the imprecision of the approximation equation (1) at the origin. The phase distribution of the components f and $2f$ expected from calculation was confirmed by the measured results.

When two sound signals of different frequencies are superposed with the stagnation point flow, because of the nonlinearity of the controlled profile, the sum and differential frequencies appear in addition to the harmonics. In the calculated approximation, the superposition of two frequencies is considered by the formulation:

$$V = V_\infty - \frac{V_\infty - V_0}{1 + b(A_1 \sin \omega_1 t + A_2 \sin \omega_2 t + y)^2} \quad (5)$$

and as above we get for the alternating velocity:

$$\begin{aligned} v = & \frac{(V_\infty - V_0) b}{(1 + b y^2)^2} \{ 2 y (A_1 \sin \omega_1 t + A_2 \sin \omega_2 t) - \\ & - \frac{1}{2} (A_1^2 \cos 2 \omega_1 t + A_2^2 \cos 2 \omega_2 t) + \\ & + A_1 A_2 [\cos(\omega_1 - \omega_2) t - \cos(\omega_1 + \omega_2) t] \}. \quad (6) \end{aligned}$$

4. Acoustic Excitation of Boundary Layer Waves

In the transition from a laminar to a turbulent flow boundary layer, boundary layer waves develop whose amplitude increases with the distance traveled. These unstable boundary layer waves are the cause of developing turbulence in the boundary layer. This problem was first treated theoretically by Tollmien and Schlichting [3]. The calculations solved the Navier-Stokes equations for incompressible flow with the boundary conditions of the flow boundary layer and the perturbation formulation for the boundary layer waves:

$$\begin{aligned}\psi(x, y, t) &= \varphi(y) e^{j(\omega t - kx)} = \\ &= \varphi(y) e^{-j(\beta + j\alpha)x} e^{j\omega t}\end{aligned}\quad (7)$$

1328

Here k is the complex wave number $\beta + j\alpha$ and ω is the angular frequency of the perturbation. From the definition of the current function, it follows that the alternating velocities v_x and v_y are:

$$\begin{aligned}v_x &= \frac{\partial \psi}{\partial y} = \frac{\partial \varphi}{\partial y} e^{j(\omega t - kx)} \\ v_y &= -\frac{\partial \psi}{\partial x} = jk\varphi(y) e^{j(\omega t - kx)}.\end{aligned}$$

With a given frequency ω and a Reynolds number $Re = \frac{V_\infty \delta^*}{\nu}$ (δ^* = displacement thickness; ν = kinematical viscosity), one gets from the calculation the wavelength and amplitude coefficient of the perturbation. The additional requirement $\alpha = 0$ yields the curve of neutral stability separating the regions of stable and unstable boundary layer waves. Only boundary layer waves with frequencies in the instability region ($\alpha > 0$) cause turbulence.

The same conditions also apply for the boundary layer waves generated by sound control at the stagnation point. An amplification can only be expected if the frequency and Reynolds number

(or wind velocity) are so selected that the amplitude coefficient α is > 0 .

To study this behavior, the alternating velocity was measured a short distance above the plate, using the hot-wire anemometer. The anemometer was moved at a constant speed in the α direction. Here three velocity components are superposed:

1. The profile control at the stagnation point
2. The velocity of the boundary layer wave
3. The particle velocity.

Outside the stagnation point, only components 2 and 3 appear, and differ by their phase velocity (the phase velocity of the boundary layer wave is ca. $0.35 V_\infty$ and is thus less than 1% of the speed of sound c_0 in the measurement region). The superposition of these two components leads to a waviness of the velocity curve, from which at the known speed of sound c_0 the phase velocity and amplitude exponent α of the boundary layer wave can be determined.

Fig. 5. Excitation of boundary layer waves by acoustic superposition. The measurement curves show the superposition of the particle velocity on the velocity of the boundary layer wave, which increases sharply at higher wind velocities. $f = 1.8$ kHz.

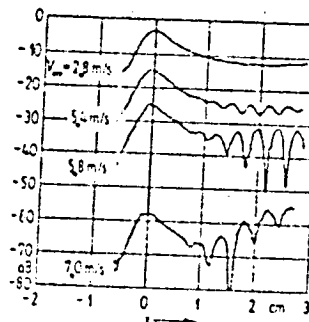


Figure 5 shows recordings of such velocity distributions. The frequency is chosen so that as the wind velocity rises the boundary layer wave becomes more and more unstable (the ordinate in Fig. 5 is scaled logarithmically, the individual curves are offset from each other).

As was shown in Section 3, with control by two signals of

different frequencies, the sum and differential frequencies also appear. If for example the frequencies f_1 and f_2 are selected so as to lie above the instability region, but the difference Δf is in the instability region, then only one boundary layer wave with the frequency Δf proceeds from the stagnation point. From Eq. (6) one expects the velocity of the differential frequency wave to be proportional to the product of the amplitudes of f_1 and f_2 (A_1 and A_2). For an amplitude range $20 \log A_1 A_2 > 40$ dB, this relationship was confirmed (with an accuracy of $\pm 3\%$).

To verify all boundary layer waves of the mixed products as generated with stagnation point control, a short traveling section with a pressure increase was set up behind the stagnation point, where all the boundary layer perturbations were greatly amplified. Thus even the higher products assumed measurable amplitudes. Table I shows the boundary layer wave frequencies thus verified, in Hz:

Table I
Calculated and measured boundary layer waves

Wellenart ^a	Wellenfrequenzen b	
	berechnet ^c Hz	gemessen ^d Hz
f_1	—	1230
f_2	—	1840
$2f_1$	2460	2470
$2f_2$	3680	3660
$f_1 + f_2$	3070	3050
$f_1 - f_2$	610	640

Key: a. kind of wave
c. calculated

b. wave frequencies
d. measured

5. Suppression of Turbulence

Above it was shown that sound control at the stagnation point can excite boundary layer waves and thus increase boundary layer turbulence. Moreover, by beaming in a sound signal at a frequency above the instability region, it is possible to

ORIGINAL PAGE IS
OF POOR QUALITY

suppress perturbations arising from the stagnation point, and thus force a laminar form of the boundary layer.

/329

The perturbation of the flow toward the stagnation point, which leads to a turbulent boundary layer on the measurement plate, was induced at low wind velocities by an obstacle in the lower part of the channel; at higher wind velocities, an instability of the stagnation point flow developed spontaneously.

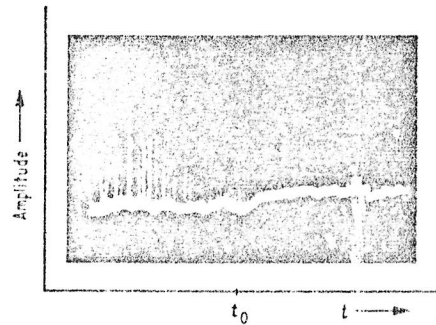
To study the effects of sound irradiation upon the development of the boundary layer, the following variables were used:

1. The position of the transition point,
2. The degree of turbulence of the boundary layer at a fixed point x ,
3. The amplitude exponent of the perturbation in the laminar-turbulent transition region.

The dependence of these values upon the frequency and amplitude of the sound signal, wind velocity and size of the preceding perturbation was studied.

It developed that above a certain frequency (which depends on wind velocity), perturbation is suppressed more and more strongly as the signal amplitude increases. At low perturbation, complete suppression can be achieved. Figure 6 shows an oscillographic photo of this turbulence suppression. At time t_0 , the sound signal was switched on. The turbulence jumps disappear almost completely.

Fig. 6. Turbulence suppression by sound irradiation (screen photo of turbulence velocity).



The results obtained by the various measurement methods given above were in agreement.

Fig. 7. Change in amplitude exponent of turbulent flow with superposition of a sound signal with frequency f .

Key: a. change in amplitude exponent
b. signal frequency

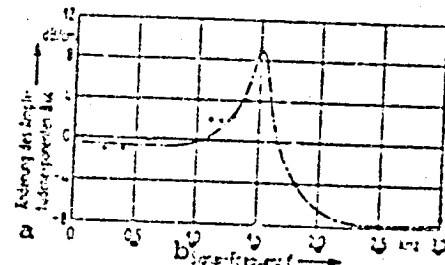


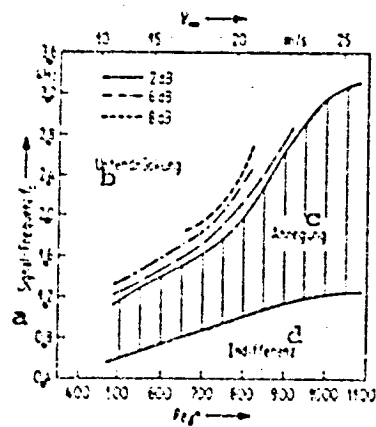
Figure 7 shows the change in the amplitude exponent of the natural perturbation in the transition region, as induced by sound irradiation. The wind velocity is 10 m/s. The particle velocity is constant for all frequencies. Three regions are distinguished. In the medium frequency range the perturbation is amplified. Here, as explained above, the sound irradiation generates boundary layer waves that amplify the natural perturbation. At low frequencies the sound field has no influence on the development of turbulence. At frequencies above the excitation range, however, the amplitude exponent of the perturbation is greatly reduced; turbulence is suppressed. The change of -8 dB/cm corresponds to complete suppression.

In comparing the boundaries of the instability region in Fig. 7 with the theory, the exact course of the outer flow must be taken into account. In the present case the outer flow presents a slight pressure increase. From the change in the middle velocity dU_∞/dx and in the boundary layer thickness δ , one gets a profile parameter $\sigma^2 \frac{dU_\infty}{dx}$ of ca. 3 to 4. For these values the agreement with theory is satisfactory [4].

The same considerations apply for the measurements in Fig 8, which graphs the boundaries of the excitation and turbulence suppression regions for the wind velocity range 10 to 30 m/s ($Re = 400$ to 1000). Here too the particle velocity is constant

Fig. 8. Frequency ranges of turbulence amplification and suppression.

Key: a. signal frequency
b. suppression
c. excitation
d. neutral stability



for all velocities and frequencies (the dotted lines in the suppression region give the change in the degree of turbulence at a fixed location x). The difference in the stability boundaries in Figs. 7 and 8 results from a different measurement setup.

Insight into the mechanism of turbulence suppression is provided by the studies in which an instability in the stagnation point flow was produced by increasing the wind velocity. Here positionally fixed vortices developed ahead of the front plate edge, and acted as starting points for boundary layer perturbation.

This perturbation was measured precisely with two hot-wire anemometers, and the spatial phase and amplitude distribution was determined. These measurements showed that these are positionally fixed vortices. The fundamental frequency of this perturbation plus the velocity of the outer flow and the diameter of the rounding of the front plate edge yields a Strouhal number

$$\text{Str} = 0.21 \pm 10\%$$

which at the present Re numbers is concordant with values in the literature.

Fig. 9. Frequency change of natural vortex due to acoustic superposition (entrainment).

Key: a. frequency ratio
b. signal frequency
c. signal amplitude

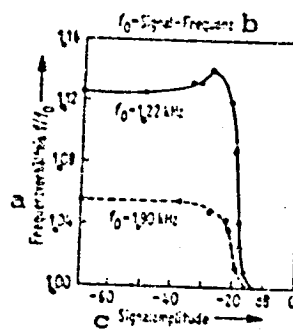


Fig. 10. Suppression of natural vortex due to superposition of a sound signal of very different frequency.

Key: a. perturbation amplitude
b. signal amplitude

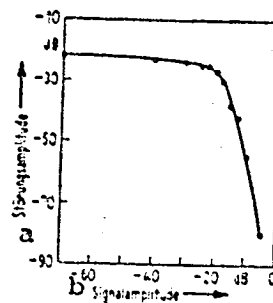
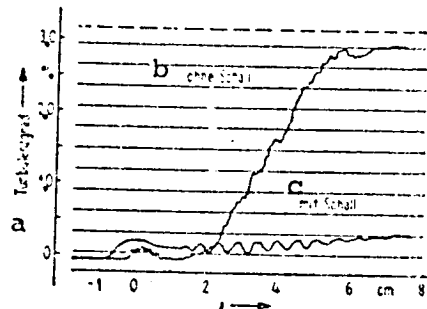


Fig. 11. Development of turbulence in direction of flow with and without acoustic superposition.
 $x = 0$: stagnation point.
Signal frequency 4 kHz.

Key: a. degree of turbulence
b. without sound
c. with sound



If a sound signal is now superposed on this natural vortex, a synchronization of the vortex is observed if the sound frequency and vortex frequency are close together. As the sound amplitude increases the vortex frequency approaches closer and closer to that of the sound signal (Fig. 9, f_0 is the signal frequency). At a greater frequency separation of the two perturbations, no further synchronization occurs. Now the natural perturbation is completely suppressed, if the amplitude

of the sound signal is great enough. (Fig. 10 shows the decrease in the intensity of the natural vortex as the signal amplitude increases.) If the sound frequency is above the instability range, the cause of turbulence in the boundary layer is thus eliminated and replaced by a non-critical perturbation. This shifts the transition point to higher Re numbers (or longer distances traveled). Finally, Fig. 11 shows an example of turbulence suppression. This is a level recording of the degree of turbulence 0.5 mm away from the plate surface as a function of the distance traveled x ($x = 0$ is the front edge of the plate). While a steep increase in turbulence occurs at $x = 3$ cm without sound superposition, with sound superposition the boundary layer remains laminar. The degree of turbulence increases only slowly (1 dB/cm compared to 12 dB/cm without sound signal). The distance traveled from the start of the plate to a completely turbulent boundary layer is five times as great with sound superposition.

This work was performed under Contract No. AF 61(052)-666 AFSC, European Office, Office of Aerospace Research, United /331 States Air Force, Brussels.

The authors wish to thank Prof. E. Meyer for his supportive interest in the work.

(Received 25 November 1963)

REFERENCES

- [1] Le Conte, J., Phil. Mag. 15 (1858), 235.
- [2] Chanaud, R.C. and Powell, A., Experiments concerning sound sensitive jet. J. Acoust. Soc. Amer. 34 (1962), 907.
- [3] Schlichting, H., Grenzschichttheorie [Boundary Layer Theory]. G. Braun, Karlsruhe, 1968, Chapter XVI.
- [4] Schlichting, H., op. cit., Chapter XVII.

END

DATE

FOLMED

JUN 2 1986



3 1176 01355 7948

DO NOT REMOVE SLIP FROM MATERIAL

Delete your name from this slip when returning material
to the library.

NAME	DATE	MS
<i>Langley Research Center</i>	<i>3/3/93</i>	<i>J-10</i>
<i>L. Johnson</i>		<i>125</i>

NASA Langley (Rev. Dec. 1991)

RIAD N-75